The Cerebral Basis of Mapping Nonsymbolic Numerical Quantities onto Abstract Symbols: An fMRI Training Study

Ian M. Lyons[1,2] and Daniel Ansari[1,3]

Abstract

■ Although significant insights into the neural basis of numerical and mathematical processing have been made, the neural processes that enable abstract symbols to become numerical remain largely unexplored in humans. In the present study, adult participants were trained to associate novel symbols with nonsymbolic numerical magnitudes (arrays of dots). Functional magnetic resonance imaging was used to examine the neural correlates of numerical comparison versus recognition of the novel symbols after each of two training stages. A left-lateralized fronto-parietal network, including the intraparietal sulcus, the precuneus, and the dorsal prefrontal cortex, was more active during numerical comparison than during perceptual recognition. In contrast, a network including bilateral temporal–occipital regions was more active during recognition than comparison. A whole-brain three-way interaction revealed that those individuals who had higher scores on a postscan numerical task (measuring their understanding of the global numerical organization of the novel symbols) exhibited increasing segregation between the two tasks in the bilateral intraparietal sulci as a function of increased training. Furthermore, whole-brain regression analysis showed that activity in the left intraparietal sulcus was systematically related to the effect of numerical distance on accuracy. These data provide converging evidence that parietal and left prefrontal cortices are involved in learning to map numerical quantities onto visual symbols. Only the parietal cortex, however, appeared systematically related to the degree to which individuals learned to associate novel symbols with their numerical referents. We conclude that the left parietal cortex, in particular, may play a central role in imbuing visual symbols with numerical meaning. ■

INTRODUCTION

The capacity to represent and manipulate numerical magnitudes in symbolic format is a critical prerequisite for any complex, culturally determined mathematical system (Dehaene, 1997). Recent years have seen a number of inquiries into the neural substrates of numerical processing. The majority of these studies have examined the neural correlates of tasks involving mental manipulation of Arabic numerals or number words (for an overview, see Dehaene, Piazza, Pinel, & Cohen, 2003). However, the cerebral bases of how visual symbols acquire numerical meaning remain largely unexplored.

More precisely, the question of how external representations of number (Arabic numerals and number words) are mapped onto internal representations of numerical magnitude has yet to be explicitly addressed in humans at the neural level. Much like phonemes need to be mapped onto graphemes to enable reading, quantities need to become symbolic to enable more efficient and complex arithmetic (Price & Mechelli, 2005). In contrast to letters, however, a numeral need not contain phonetic information per se, and association between the symbol and its referent may be possible through direct grapheme–semantic mappings. Greater insights into the processes by which symbols could become numerical will aid, for example, in further understanding the neural basis of numerical cognition and may prove informative for the study of the neural correlates of typical and atypical number development.

One method for understanding how numerical symbols acquire their semantic meaning is to take a developmental approach and study the emergence of symbolic number representations in the developing brain (Ansari, Garcia, Lucas, Hamon, & Dhital, 2005; Rivera, Reiss, Eckert, & Menon, 2005). Although informative, there exists great variability in the degree to which children have experience with and exposure to numerical symbols and the magnitudes they represent. A different approach is to train adult individuals to associate artificial symbols with numerical magnitudes and to measure the behavioral and neural responses underlying this mapping process. Artificial training sets have been used successfully to identify neural mechanisms thought to underlie specific cognitive skills in a variety of domains, (e.g., Van Opstal, Verguts, Orban, & Fias, 2008; Xue, Chen, Jin, & Dong, 2006; Bitan, Booth, et al., 2005; Bitan, Manor, Morocz, &

[1]Dartmouth College, [2]University of Chicago, [3]University of Western Ontario, Canada

Karni, 2005; Callan, Callan, & Masaki, 2005; Forkstam & Petersson, 2005; Siok, Perfetti, Jin, & Tan, 2004; Gauthier, Tarr, Anderson, Skudlarski, & Gore, 1999; Gauthier, Williams, Tarr, & Tanaka, 1998). In the present study, we used artificial numerical symbols to study the neural processes underlying the learning of the mapping between abstract symbols and numerical magnitudes. To do so, we generated an artificial set of distinctive, two-dimensional visual shapes (see Figure 1) and, subsequently, trained healthy adult subjects to associate these shapes with approximate numerical quantities. Several theories (Dehaene, 2008) and computational models (Verguts & Fias, 2004; Dehaene & Changeaux, 1993) have proposed that numerical symbols acquire their meaning through being mapped onto nonsymbolic representation of numerical magnitude. The present study therefore provides an experimental simulation of this proposed developmental process. This approach is similar to that recently employed by Diester and Nieder (2007) to study the representation of numerical symbols in the nonhuman primate brain, where monkeys were trained to associate Arabic numerals with nonsymbolic numerosities. Such simulations can provide important insights into processes involved in symbol-referent mappings, although this depends crucially on the validity of the assumption that numerical symbols acquire their meaning by being mapped onto nonsymbolic numerical magnitudes (Ansari, 2008).

After each of two stages (to enable the measurement of any learning-related effects) of symbol training, during which participants associated novel numerical symbols with nonsymbolic numerosities, subjects compared symbols in terms of the numerical magnitudes they represented. To identify brain regions involved in the processing of visual characteristics of the novel symbols, participants also completed a perceptual recognition task. This task required subjects to identify which of two highly similar symbols was part of the training set (see Figure 2), thereby matching the perceptual and response-selection requirements of the experimental task, while not requiring explicit access to the numerical quantities associated with the novel symbols.

By directly contrasting neural activity during the numerical comparison relative to the recognition task, the brain regions associated with explicitly accessing the newly associated referents of the novel symbols can be revealed. Because a novel set of symbols was used, and because participants were trained only to associate numerical information with these symbols, the brain regions revealed in this way may be said to be involved in the explicit semantic processes related to numerical symbol acquisition. Furthermore, the reverse contrast (recognition > numerical comparison) allowed for the identification of regions more involved in the recognition and perceptual discrimination of these symbols. Thus, these contrasts will reveal the brain regions involved in both the semantic and perceptual processing of the novel symbols. In addition to the group-based factorial analysis, we included an individual differences approach to the analyses. That is, at the whole-brain level, we examined the data for brain–behavior correlations to assess individual differences in learning trajectories.

Against the background of numerous studies pointing to central involvement of regions in the inferior parietal lobe and the intraparietal sulci during processing of highly enculturated numerical symbols (e.g., Piazza, Pinel, Le Bihan, & Dehaene, 2007; Ansari et al., 2005), we predicted that inferior parietal regions would be involved in the numerical comparison of the novel symbols to a greater degree than in the recognition task. Furthermore, we anticipated that these cortical regions would assume a greater role in the processing of novel numerical symbols as a function of training (i.e., greater activation after the second stage of training). In addition, given the involvement of the lateral temporo-occipital junction in processing complex visual objects, including recognition of written words (McCandliss, Cohen, & Dehaene, 2003), we hypothesized that this region would be more involved in perceptually recognizing the symbols.

METHODS

Participants

Participants were 21 right-handed, neurologically normal undergraduate and graduate students (13 women) from Dartmouth College, New Hampshire, ranging in age from 18.9 to 27.3 years (mean = 21.1 years). One subject did not perform above chance on the postscan ordering

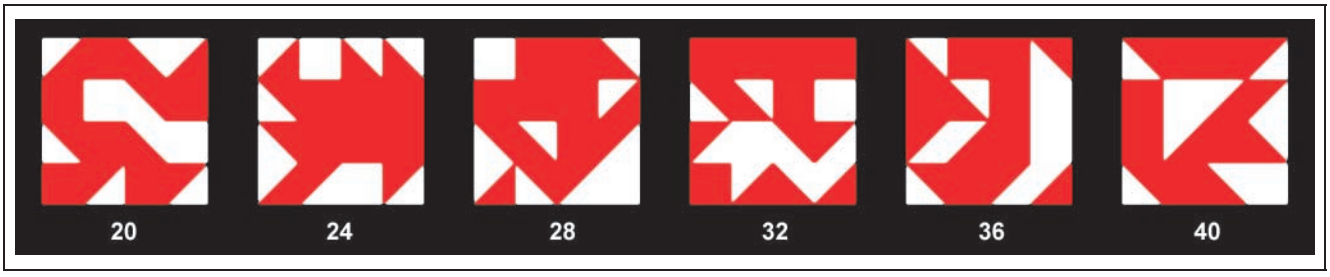

Figure 1. The six experimental symbols: Numbers in white indicate the number of dots associated with each symbol. Note that the same number of dots was presented with a given symbol for the duration of the experiment.

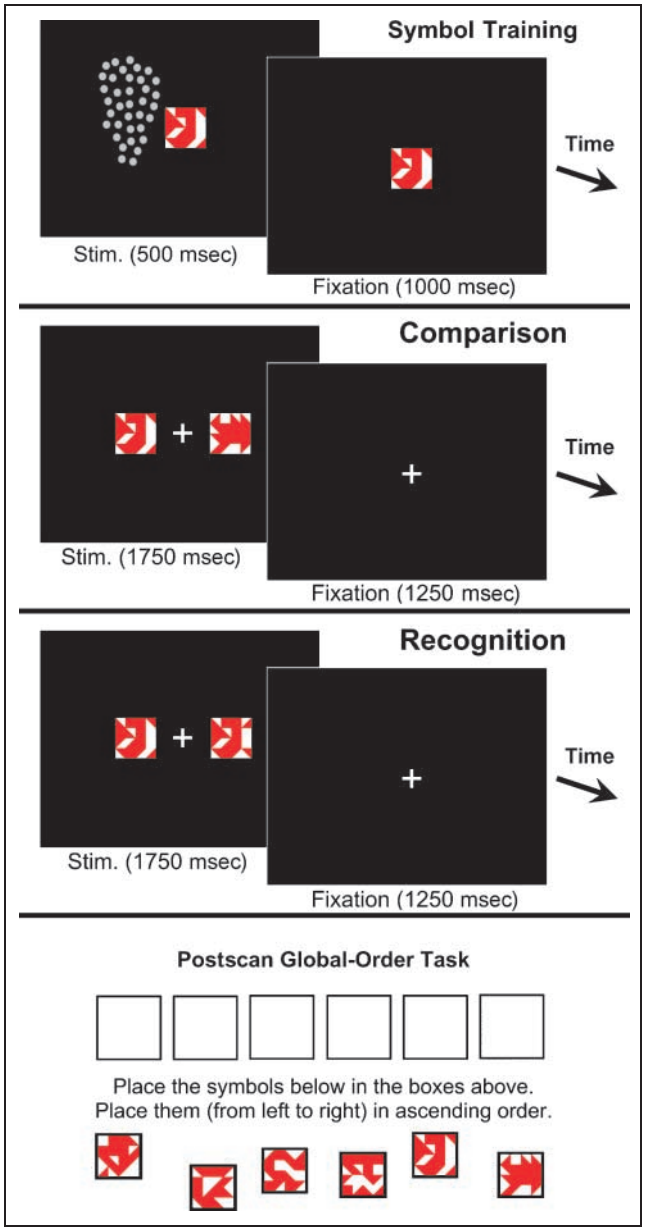

Figure 2. Symbol training and experimental tasks. The top panel provides an example of one trial from the symbol-training session. Participants viewed nine trials for a block. Throughout a block, one symbol served as the fixation point; nine dot arrays of a given number where then presented around the symbol. Participants were not required to make any responses during symbol training. The second panel shows an example of the numerical comparison task. Six trials were presented per block. If a participant judged the symbol on the left or right to represent the larger quantity, they were to press a button with their corresponding hand. Responses were accepted for the full 3-sec duration of the trial; participants were informed of this fact. The third panel shows an example of the recognition task. If the subject judged the symbol on the left or right to be exactly the same as the one from the training set, then they were to press a button with their left or right hand, respectively. Responses were collected as in the comparison task. The bottom panel depicts the postscan global-ordering task. The symbols were presented as six laminated chips. The symbols were presented as a stack that had previously been randomly hand-shuffled. Subjects were asked to rearrange the chips by placing one in each box, ordered (from left to right) in terms of the numerical magnitudes they represented.

task (see below), and thus, was omitted from further analysis (therefore, all analyses reported below included a total of 20 participants). Written consent for participation in the experiment was obtained from all participants. The experimental procedure and consent form were approved by the Committee for the Protection of Human Subjects at Dartmouth College.

Stimulus Design

Symbolic Stimuli

Participants were instructed to associate quantities of dots (presented in arrays) with novel stimuli. These stimuli (hereafter referred to as ''symbols'') consisted of six red [RGB = (255, 0, 0)] and white [RGB = (0, 0, 0)] squares. Each square was 80 × 80 pixels in size and comprised of sixteen 20 × 20-pixel contiguous sections. Sections were one of six red and/or white geometric shapes: a red square (6 per stimulus), a white square (2 per stimulus), or one of four permutations of a diagonally bisected red-and-white square (2 each per stimulus). Novel symbols were generated using a program written in Director MX (Macromedia, San Francisco, CA) that randomly arranged the appropriate number of each of these sections into an 80 × 80-pixel square. Sixty-four such stimuli were initially created. Pilot testing was used to determine the six symbols used in the actual experiment (shown together in Figure 1), in which six participants rated the six most distinguishable symbols. Only those symbols rated in the top six by four of six pilot participants were used in the actual experiment.

Prescan Practice

Before entering the scanner, participants were instructed verbally about the nature of the experimental tasks. During a period of 2 min, participants were explicitly told to learn to recognize the six experimental symbols on the basis of their visual features alone (at this point in the experiment, no dot–quantity associations had been presented). Participants were then asked to identify the six experimental symbols from a randomized set containing 12 additional lure symbols; all subjects successfully completed this task before entering the scanner.

During the acquisition of the co-planar anatomical scan, subjects practiced associating dot quantities with three practice symbols. The three practice symbols were the same size and color as the experimental symbols but were designed using simple, symmetrical combinations of ASCII punctuation characters so as to further avoid any confusion between symbols used during practice and those used during the actual experiment. Participants learned to associate these practice symbols with four, six, and eight dots, and were told repeatedly that these were merely *practice* symbols (i.e., that they would not see them again after the practice session).

During acquisition of the high-resolution anatomical scan, participants practiced the comparison and recognition tasks (see Figure 2 and Procedure below) using the three practice symbols.

Following the practice session, to ensure maximum exposure to the perceptual features of each experimental symbol (and to further avoid confusion as to which symbols were to be used in the actual experiment), participants watched a slide show of these experimental symbols (i.e., those shown in Figure 1). Symbols were presented individually in randomized order for 45 sec each in the center of a black background without any accompanying dots (participants were informed of this randomization).

Novel Symbol-training Stimuli

During symbol training, a symbol was positioned in the center of a 1024 × 768-pixel black background. Symbol size and orientation were fixed throughout the experiment. Participants saw an array of light gray [RGB = (206, 206, 206)] dots randomly arranged around a given symbol (Figure 2, top). All arrays were unique with respect to dot location. Dots displayed around symbols numbered 20, 24, 28, 32, 36, and 40 (Figure 1); this number was held constant for each symbol throughout the experiment. However, at no point in the experiment were participants explicitly informed of the number of dots associated with any of the symbols. Presentation of each symbol-training array lasted 500 msec; therefore, participants could not have counted the dots and had no means of forming an association between a symbol and the correct, *exact* quantity of dots with which it was presented. In this way, participants can only have formed an *approximate* representation of the number of dots associated with any of the symbols.

To ensure the number of dots presented around a given symbol was uniquely specified by the numerical quantity of dots, related continuous variables were controlled for. Specifically, the area of individual dots, aggregate (i.e., all dots in a slide combined) perimeter, and aggregate area were each equated across one-third of all dot arrays. If, for example, individual dot size was held constant between symbols (i.e., regardless of the number of dots in an array), then the aggregate perimeter and the aggregate area would cospecify dot numerosity for each symbol. To control for this, individual dot size was held constant across symbols only for one third of all dot arrays. Dot sizes for the remaining two-thirds of symbol-training arrays for a given symbol were adjusted for each display such that the aggregate area and perimeter, respectively, were equated across all symbols, and thus, no longer reliably cospecified numerosity. For a given array, all dots were of equal size. Overall (across all arrays for all symbols), dot sizes ranged from 26 to 106 pixels in diameter (viewing angle ≈ 1° to 6°). In addition, for all dot displays, the minimum and maximum distance between individual dots was held constant, thus ensuring that relative local densities did not covary exclusively with numerical quantity (i.e., the average local distance between two neighboring dots was held constant across symbols, such that the average proximity between adjacent dots could not be used to infer numerosity). Dots were not permitted to overlap with the centrally located symbol. Within the constraints of the aforementioned parameters, dot locations were randomly determined for each slide (36 training slides in total for each symbol). In this way, across all dot arrays presented with a given symbol, no horizontal or vertical bias could have been formed on the basis of average dot location for any given symbol. Finally, all dot arrays were presented only once over the course of the entire experiment to ensure that participants could not have relied on strategies such as dot-pattern recognition to distinguish the symbols.

Test Stimuli

After symbol training, participants completed a numerical comparison and a recognition task using the symbols they had seen during training (see Table 1). For the comparison task (Figure 2, second panel), two of the experimental symbols were presented on either side of a white fixation cross (the quantitatively greater symbol appeared on the left and right sides equally often); for the recognition task (Figure 2, third panel), one of these symbols was presented on one side of the fixation cross, and a modified version of this *same* symbol was presented on the opposite side. For the recognition task, modified symbols were created by randomly switching two of the 16 components that comprised the original symbol. None of these ''foil'' symbols was ever presented more than once throughout the entire experiment (the side of foil presentation was counterbalanced

Table 1. Overview of Experiment Procedure

Time		
	Practice, Anatomical Scans	
	Stage One	1 Run Symbol Training
		2 Runs of Comparison & Recognition Tasks
	Rest (DTI Scan)	
	Stage Two	3 Runs Symbol Training
		2 Runs of Comparison & Recognition Tasks
	Post-Scan Global Ordering Task	

across trials). Symbols were presented at a distance of 345 pixels (viewing angle ≈ 20°) from one another.

Stimulus Presentation

Practice and experimental stimuli during scanning were presented using SuperLab 4.0 (Cedrus Corporation, San Pedro, CA). Stimuli were projected (Epson 7000 color projector) onto a rectangular mirror (9.7 cm × 12.7 cm) set approximately 10 to 12 cm (depending on individual head size) from the subject using a 59-Hz refresh rate at 1024 × 768 resolution (viewing angle ≈ 60–65°). TR-onset triggered the beginning of each block directly, thus ensuring stimulus presentation and TR acquisition synchronization.

Procedure

Table 1 provides a timeline of the experimental procedures. Figure 2 shows example stimuli as well as trial timing information for trials used during symbol training, and the numerical comparison and recognition tasks. Symbol-training blocks lasted 13.5 sec (9 consecutive trials per block with 15 sec fixation/rest between blocks), and test blocks lasted 18 sec (6 consecutive trials per block also with 18 sec fixation/rest between blocks).

Symbol Training and Test Procedures

All functional and anatomical runs were acquired in a single scanning session divided into two stages (see Table 1). In the first stage, participants completed an initial symbol-training phase. This part of the procedure consisted of a single cycle in which participants saw each experimental symbol once, presented in blocked fashion. Each block consisted of nine dot arrays (in nine separate displays) presented around the same symbol (arrays were counterbalanced for the three control parameters discussed above). Each display was presented for 500 msec (interstimulus interval = 1000 msec). Block (and thus symbol) orders were pseudorandomized across subjects. Participants made no responses during training; instead, they were instructed to associate a given symbol with the approximate quantity of dots shown around it.

The symbol-training phase was followed by a test phase that consisted of two functional runs. In each run, participants completed four blocks of trials (two each for the comparison and recognition tasks); block order was counterbalanced across runs. For both tasks, each trial consisted of a test pair (presented for 1750 msec) followed immediately by fixation (1250 msec). Three seconds prior to each block of trials, a brief warning was flashed to indicate trials of which task type were about to follow. This warning flash was not modeled as part of the active task blocks.

Stage 2 was identical to Stage 1, with the exception that participants viewed three training cycles instead of one. Each of these cycles (as with the first stage) contained one trial block for each symbol, with block order pseudorandomly counterbalanced across cycles. The order of symbol-training cycles was counterbalanced across subjects, as were functional runs containing the comparison and recognition tasks. This second symbol-training phase was immediately followed by a second test phase consisting of two functional runs.

Postscan Global-order Task

After exiting the scanner, participants were given unlimited time to physically arrange the six experimental symbols, increasing from left to right, in terms of the quantity each was thought to represent. More precisely, subjects were given the symbols as six small (∼2 cm^2) laminated squares in a randomly mixed fashion. They were then given a sheet of paper with six boxes arranged horizontally across the paper. They were asked to place the symbols, one in each box, with the numerically smallest symbol in the leftmost box, and increasing to the numerically largest symbol in the rightmost box. Performance on this task was calculated as follows: 1 point was awarded for each correctly (correct numerical order) specified relative pair of the novel symbols; this total was then divided by the total number of such pairs (15). (Example: If one responded with A–C–B for a set that was, in fact, correctly ordered as A–B–C, then the B–C pair would be scored as incorrect: 2 correct out of 3 possible pairs would yield a score of 0.67.) Using this formulation, chance performance would receive a score of 0.5; perfect performance would yield a score of 1.0. The task is depicted in the bottom panel of Figure 2.

fMRI Acquisition and Analysis

Functional and structural images were acquired in a 3-T Phillips Intera Allegra whole-body MRI scanner (Phillips Medial Systems, The Netherlands) using an eight-channel Phillips Sense head coil. A gradient echo-planar imaging T2*-weighted sequence sensitive to blood-oxygenation level-dependent (BOLD) contrast was used to acquire 30 functional slices per volume (3 mm thickness; 0.5 mm gap; 80 × 80 matrix; repetition time = 2500 msec; echo time = 35 msec; flip angle = 90°; field of view = 240 × 240 mm) covering the whole brain; test-session runs consisted of 68 volumes each. High-resolution anatomical images were acquired using three-dimensional, whole-brain T1-weighted images (160 slices) in the sagittal plane (1 × 0.94 × 0.94) with a standard Phillips MP-RAGE 3-D sequence.

All preprocessing steps and analyses were conducted using BrainVoyager QX, version 1.8.6 (Brain Innovation, Maastricht, Netherlands). Preprocessing of data

included slice scan-time correction, correction for three-dimensional head motion, mean intensity adjustment at the volume level to correct for scanner-related fluctuations, linear trend removal, spatial smoothing using a 6-mm full width at half maximum Gaussian kernel, and temporal high-pass filtering to remove nonlinear drifts of three cycles or fewer per time course. Following initial automatic alignment, the alignment of subjects' functional images to their corresponding high-resolution structural image was manually fine-tuned. The realigned functional dataset was then transformed into Talairach space (Talairach & Tournoux 1988). A two-gamma hemodynamic response function (Friston et al., 1998) was used to model the expected BOLD signal.

Group-level Analysis

Analysis of the BOLD signal was based on a multiple regression analysis of each functional time series (Friston et al., 1995). A general linear model (GLM) was used to perform a group-level random effects analysis. Results from the GLM were submitted to a whole-brain 2 (task: comparison, recognition) by 2 (stage) ANOVA. Maps were created showing significant voxels for both main effects and the Task-by-Stage interaction. These maps were thresholded at $p < .001$ and subsequently corrected for multiple comparisons using cluster-size thresholding (Goebel, Esposito, & Formisano, 2006; Forman et al., 1995). In this method, an initial voxel-level (uncorrected) threshold is set. Then, thresholded maps are submitted to a whole-slab correction criterion based on the estimate of the map's spatial smoothness and on an iterative procedure (Monte Carlo simulation) for estimating cluster-level false-positive rates. After 1000 iterations, the minimum cluster size that yielded a cluster-level false-positive rate (α) of .01 (1%) or less was used to threshold the statistical maps. Significant clusters from this analysis were thus limited to clusters of six or more contiguous functional voxels.

Individual Performance Differences and Brain Activation

Despite including only subjects who performed above chance on the comparison, recognition, and postscan ordering tasks, large individual differences were observed both in terms of initial performance (after only one stage of symbol training) and in terms of the degree of improvement following the second round of training. By averaging over activity in individuals with highly varied behavioral performance, important effects of individual differences in learning on brain activation may not be detected. Thus, in addition to these group-based analyses, we examined whether the activity of specific brain regions was significantly related to behavioral performance. For each of the individual difference analyses described below, maps were thresholded at $p < .001$ and cluster-level corrected at $\alpha = .01$.

As the central index of performance, we used the postscan global-order task. This task was the only instance where participants worked with all symbols at the same time after learning to recognize and associate them with dot quantities (i.e., after symbol training). Thus, this task may be viewed as a measure of subjects' global representations of the symbols as part of a numerically related set. Moreover, this task was performed outside of the scanner after all other tasks had been completed. As such, this task was seen both as relatively neutral with respect to the task being performed during signal measurement and as a particularly stringent test of the relation between neural activity and subjects' ability to recognize and understand the symbols' numerical meaning. We tested whether postscan accuracy interacted with each of the three ANOVA measures (i.e., main effects of task and stage, and the Task-by-Stage interaction).

We were also interested in whether changes in performance during each of the tasks performed in the scanner (numerical comparison and perceptual recognition) related to changes in neural activity recorded during that task. To assess whether changes in performance related to changes in neural activity, two regression maps were generated for each task (one for each behavioral measure). For a given task and a given measure, the difference between Stage 1 and Stage 2 performance was regressed on the contrast of Stage 2 > Stage 1 neural activity.

Finally, evidence of sensitivity to numerical distance when comparing the novel symbols, especially at the neural level, would provide additional corroborating evidence that subjects were indeed learning to use the novel symbols in a numerically meaningful manner (Pinel, Dehaene, Riviere, & LeBihan, 2001). The numerical distance effect (the larger the numerical distance between two numbers, the faster and more accurate participants are found to be at making relative magnitude judgments) is considered a key hallmark of ordered, numerical magnitude representations (Moyer & Landauer, 1967). Thus, we regressed subjects distance effects in accuracy (i.e., accuracy for far distances less accuracy for the closest distance) and response times (i.e., reaction times for the closest distance less reaction times for far distances) on neural activity during each stage of each task.

RESULTS

Behavioral Results

Responses were accepted between 300 and 3000 msec after onset of the test pair. Given the difficulty of the task (average response times greater than 1000 msec; see Table 2) and the absence of any feedback after a button press, 300 msec was seen as a reasonable cutoff for

protecting against unintentional or tardy button presses from the previous trial. Reaction times for incorrect responses were excluded from the latency analyses. Both accuracy and reaction times were analyzed in a 2 (task: comparison, recognition) × 2 (stage) ANOVA. Condition means and standard errors are summarized in Table 2A. In terms of accuracy, both main effects of task [$F(1, 19) = 44.38$, $p < .001$, $\eta_p^2 = .70$] and stage [$F(1, 19) = 68.19$, $p < .001$, $\eta_p^2 = .78$] were significant, as was the Task × Stage interaction [$F(1, 19) = 23.30$, $p < .001$, $\eta_p^2 = .55$], such that greater improvements were seen for the comparison relative to the recognition task across stages. In terms of response times, both main effects of task [$F(1, 19) = 7.07$, $p < .05$, $\eta_p^2 = .27$] and stage [$F(1, 19) = 88.78$, $p < .001$, $\eta_p^2 = .82$] were significant; however, the Task-by-Stage interaction was not [$F(1, 19) < 1$, *ns*].

For the numerical comparison task, a 2 (distance) × 2 (stage) ANOVA was carried out for accuracy and reaction times separately. Trials with ordinal distances of 1 (numerical distance of 4 in terms of represented quantity) were classified as ''small distance'' (henceforth, SD: 6 trials per participant per stage), and trials where the two presented symbols were by separated by ordinal distances of 4 or 5 (16 or 20 dots, respectively) were classified as ''large distance'' (henceforth, LD: 5 total trials per participant per stage). Distance effects for each stage were computed by subtracting SD accuracy from LD accuracy (or LD response times from SD response times) and dividing this difference by the average of the two distance scores (to control for interindividual differences in reaction time and accuracy). Condition means and standard errors are summarized in Table 2B. Analysis of the response accuracy data revealed main effects of distance, with larger distances pairs associated with more accurate performance than discrimination of symbols pairs separated by smaller distances [$F(1, 19) = 33.40$, $p < .001$, $\eta_p^2 = .64$] and stage, with increasing accuracy for both distances across stages [$F(1, 19) = 18.37$, $p < .001$, $\eta_p^2 = .49$]. The Stage × Distance interaction showed a trend toward significance [$F(1, 19) = 1.85$, $p = .19$, $\eta_p^2 = .09$]; this was due to the presence of distance effects at both stages [Stage 1: $t(19) = 3.03$, $p < .05$; Stage 2: $t(19) = 6.27$, $p < .001$]. Analysis of response times revealed significant main effects of distance [$F(1, 19) = 6.61$, $p < .05$, $\eta_p^2 = .26$] and stage [$F(1, 19) = 14.41$, $p < .001$, $\eta_p^2 = .43$], as well as a significant Distance × Stage interaction [$F(1, 19) = 5.95$, $p < .05$, $\eta_p^2 = .24$]. This interaction was driven by the presence of a distance of effect on reaction time after the second [$t(19) = 4.27$, $p < .001$] but not the first [$t(19) < 1$, *ns*] stage of symbol training.

Table 2. Condition Means for Behavioral measures (values in parentheses represent standard errors of the mean)

	Accuracy (% Correct)		*Response Time (msec)*	
	Stage 1	*Stage 2*	*Stage 1*	*Stage 2*
(A) Task				
Comparison	63.6 (3.4)	83.3 (2.5)	1386 (42)	1251 (30)
Recognition	85.2 (1.9)	91.5 (1.6)	1309 (29)	1187 (34)
(B) Distance				
Small	51.7 (4.0)	64.2 (3.7)	1380 (49)	1314 (37)
Large	70.0 (4.9)	92.0 (3.0)	1355 (55)	1165 (32)

(A) Average accuracy and response time performance for the numerical comparison and recognition tasks at each stage. (B) Average accuracy and response time performance at small and large numerical distances on the numerical comparison task.

Postscan Global-order Task

On average, performance on the postscan task was 91.0% (range = 66.7% to 100%; *SD* = 9.5%) of relative pairs correct. This suggests that, given sufficient time and the proper format in which to formulate their answers, many participants did develop a highly accurate representation of the global relations between symbols.

Neuroimaging Data

Task-by-Stage ANOVA

In the 2 (task) × 2 (stage) whole-brain, voxelwise ANOVA, 12 regions showed a significant main effect of task. Because *F* tests do not indicate directionality, we extracted the parameter estimates from each of these regions to investigate the direction of the main effect by region (see rightmost two columns in Table 3).

Comparison > Recognition. Four of these regions (see orange-colored activations in Figure 3) showed greater activation for the comparison relative to the recognition task. These regions comprised a predominantly left-lateralized fronto-parietal network, including the precuneus, the left intraparietal sulcus (IPS, BA 7), the left dorsal premotor and prefrontal cortex (PFC; spanning BA 6/8 and referred to here as the left dorsal pre-premotor cortex, or pre-PMd; Picard & Strick, 2001), and the left rostral frontal cortex (BA 10). Mean betas for the effect of task in these regions are shown in Table 3. In the left IPS, activity during both tasks was significantly above baseline ($p < .05$). In the remaining three regions, activity was above baseline for comparison but not recognition (note that activity was below baseline for recognition in left BA 10).

Recognition > Comparison. Eight regions (see blue-colored activations in Figure 3) showed greater activation for the recognition relative to the comparison task. These regions formed a predominantly bilateral parietal–occipital network, comprised of bilateral activations in

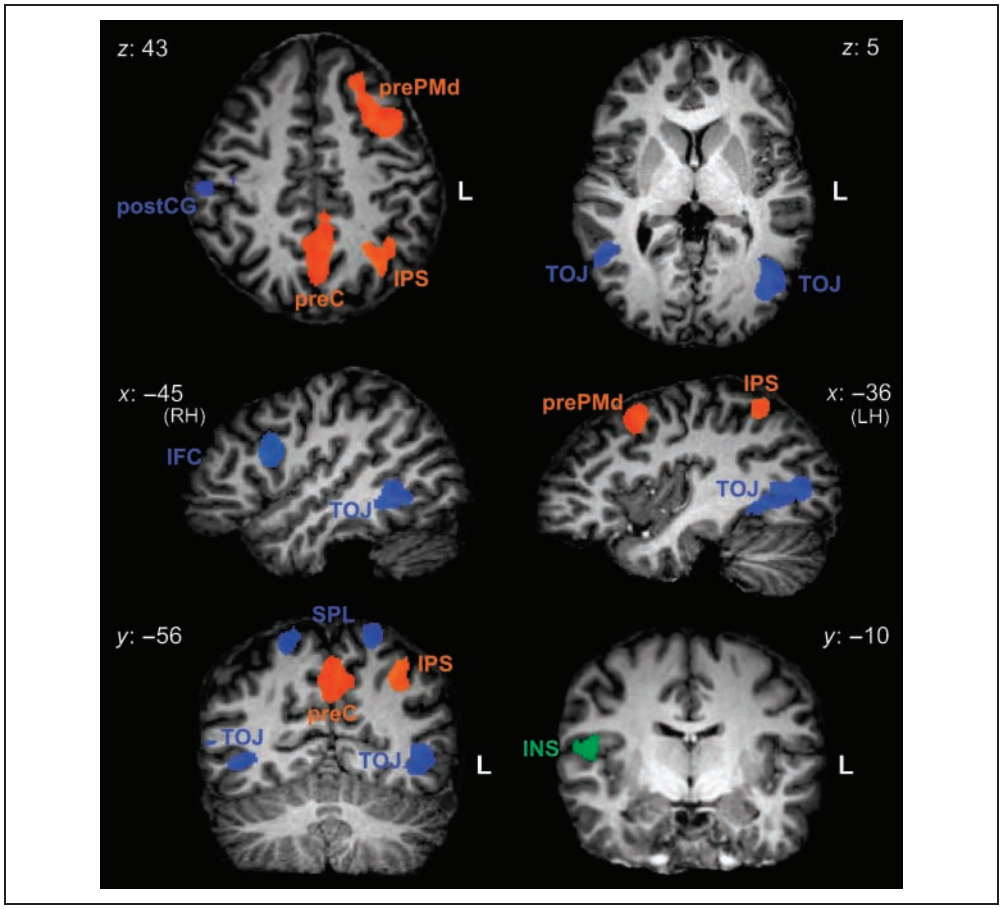

Figure 3. Regions showing a main effect of task at the whole-brain level. Brain activations displayed in orange represent brain regions that exhibited greater activation for the comparison than the recognition task, regions displayed in blue showed greater activation for the recognition than the comparison task, and regions in green showed a main effect of stage (in this case, greater deactivation during Stage 1 relative to Stage 2). Regions depicted here include the left pre-PMd (prePMd), left IPS, precuneus (preC), right IFC, bilateral TOJ, bilateral SPL, right postcentral gyrus (postCG), and right insula (INS). For a complete list of regions showing an effect of task or stage, see Table 3.

the superior parietal lobe (SPL), the occipital cortex (BA 18), and the temporal–occipital junction (TOJ). Note that both TOJ regions spanned the occipital (BA 19) and temporal (BA 37) lobes; however, the activation on the left was slightly more posterior and superior, and thus, relative to the right hemisphere region, a greater proportion of voxels lay within the occipital lobe. Two right-lateralized regions were also observed, one in the right postcentral gyrus and the other in the right inferior frontal cortex. Mean betas for the effect of task in these regions are shown in Table 3. In all regions, activity during both tasks was significantly above baseline ($p < .05$).

Effects of training stage. One region showed a main effect of stage (see Figure 3, activation colored in green), with increasing activation across stages in both tasks: right posterior insular cortex (BA 52); however, relative to baseline (see Table 3), this effect was due to decreasing deactivation. That is, activation was significantly below baseline for both stages and both tasks; the difference in stages reflected a significant change toward baseline by Stage 2, a pattern of results that may make the observed effect of stage difficult to interpret. No region showed a significant Task × Stage interaction. Region details are summarized in Table 3 and the regions are visualized in Figure 3.

Individual Differences

Relation between postscan accuracy and brain activation changes. No region showed a significant interaction between postscan ordering task accuracy and either main effect. Two regions (see green-colored activations in Figure 4), in the bilateral IPS, however, showed a significant three-way interaction between postscan accuracy, task, and stage. This effect was driven, in part, by greater activity, as a function of postscan scores, during Stage 1 for recognition versus numerical comparison [when assessing the relation between ordering scores and the contrast Rec1 > Comp1, left: $r(19) = .433$, $p = .056$; right: $r(19) = .568$, $p = .009$]; the opposite effect was seen for Stage 2, with greater activation for comparison than recognition task, and this difference was greatest for those with the highest postscan scores [left: $r(19) = .451$, $p = .047$; right: $r(19) = .369$, $p = .109$]. Put another way, the better a subject performed on the postscan global-order task, the more they tended to show a crossover interaction in these bilateral parietal regions, with greater activation for recognition in Stage 1 and greater activation for numerical comparison in Stage 2. As a function of activation change within each task, higher postscan global-order scores predicted an activation decrease in these regions for recognition [when assessing the relation between ordering scores and the

Table 3. Anatomical Regions of Interest Identified Using the Whole-brain Task-by-Stage ANOVA

Anatomical Region (Brodmann's Area)	*Center of Gravity*				*Parameter Estimates (Beta Value Activity), Mean (SE)*	
	x	*y*	*Z*	*Volume (mm^3)*	*Num. Comp.*	*Recognition*
Main Effect of Task: Comp > Rec						
L. IPS (BA 7)	−30	−52	41	2223	0.64 (0.17)	0.28 (0.16)
L. Pre-PMd (BA 6/8)	−28	14	41	3342	0.36 (0.11)	0.01 (0.11)
L. Rostral frontal cortex (BA 10)	−21	57	1	1825	0.17 (0.13)	−0.22 (0.15)
Precuneus (BA 7/31)	−1	−50	35	6330	0.37 (0.15)	−0.07 (0.13)
Main Effect of Task: Rec > Comp						
R. IFC (BA 44)	43	6	22	1551	1.20 (0.17)	1.59 (0.18)
R. Postcentral gyrus (BA 2/5)	47	−20	46	575	0.67 (0.16)	1.10 (0.16)
R. SPL (BA 7)	20	−57	53	183	2.03 (0.21)	2.42 (0.23)
R. TOJ (BA 19/37)	44	−47	−3	1016	1.14 (0.20)	1.51 (0.21)
R. Occipital cortex (BA 18)	28	−78	24	1357	2.14 (0.25)	2.47 (0.26)
L. SPL (BA 7)	−17	−56	58	213	1.73 (0.21)	2.11 (0.22)
L. TOJ (BA 19/37)	−42	−64	9	498	1.77 (0.15)	2.06 (0.15)
L. Occipital cortex (BA 18)	−28	−74	25	1280	2.17 (0.19)	2.53 (0.21)
Main Effect of Stage: S2 > S1					*Stage 1*	*Stage 2*
R. Post. insula (BA 52)	49	−10	14	306	−0.77 (0.10)	−0.36 (0.08)

The first section contains regions showing a main effect of task, with overall activity higher in the numerical comparison than the recognition task. The second section contains regions also showing a main effect of task but in the opposite direction (recognition greater than comparison). The third section contains the region showing a significant main effect of stage; this region showed overall greater activation for both tasks in Stage 2 relative to Stage 1. The rightmost two columns show mean levels of activity (beta-weights averaged across subjects) for that condition. No regions showed a Task × Stage interaction, regions showing a significant effect of task did not show an effect of stage (and vice-versa). Thus, values are included only for the factor showing a significant effect in that region (i.e., Task for the top two sections and Stage for the bottom section). Values shown in parentheses indicate standard errors of the mean (n = 20).

contrast Rec1 > Rec2; left: $r(19) = .422$, $p = .064$; right: $r(19) = .521$, $p = .019$]. No systematic linear relation was seen between comparison change and ordering scores in these regions [left: $r(19) = -.236$, $p = .316$; right: $r(19) = -.165$, $p = .487$]. Regions are visualized in Figure 4; region statistics are summarized in Table 4.

Relation between behavioral and brain activation changes. When we examined whether changes in behavioral measures (accuracy and RT) across stages for each task correlated with activation changes during completion of that task, no region was found to survive cluster thresholding at $p < .001$ ($\alpha = .01$) for either task or behavioral measure. However, at this threshold, a particularly high standardized correlation coefficient was required to reach significance [$r(19) = .693$]. As several regions of theoretical interest showed significant peak activations that exceeded this threshold, to avoid false negatives, correlation maps were rethresholded at $r(19) = .615$, $p < .005$ ($\alpha = .01$, thus requiring 7 contiguous functional voxels to reach significance). At this level, two regions showed a significant negative relation between changes in recognition task accuracy and changes in activity during this task: left inferior temporal–occipital junction (TOJi; see activation colored in pink in Figure 4) and left caudate (dorsal aspect).

In addition, a region in the left IPS showed a significant positive relation between numerical comparison accuracy changes (accuracy at Stage 2 − accuracy at Stage 1) and activity change during that task. As a reduced threshold was used in revealing these regions, interpreting their activations should be done with caution; however, it may be noted that the peak correlation voxel exceeded the stricter ($p < .001$) threshold in all three cases (left TOJi: $r = -.841$, $p = 7E{-}6$; left caudate: $r = -.766$, $p = .0002$; left IPS: $r = .713$, $p = .0006$). Regions are shown in Figure 4 and summarized in Table 4. No regions were found to show a significant relationship between changes in reaction time and changes in fMRI signal change for either task, even at the reduced threshold of $p < .005$.

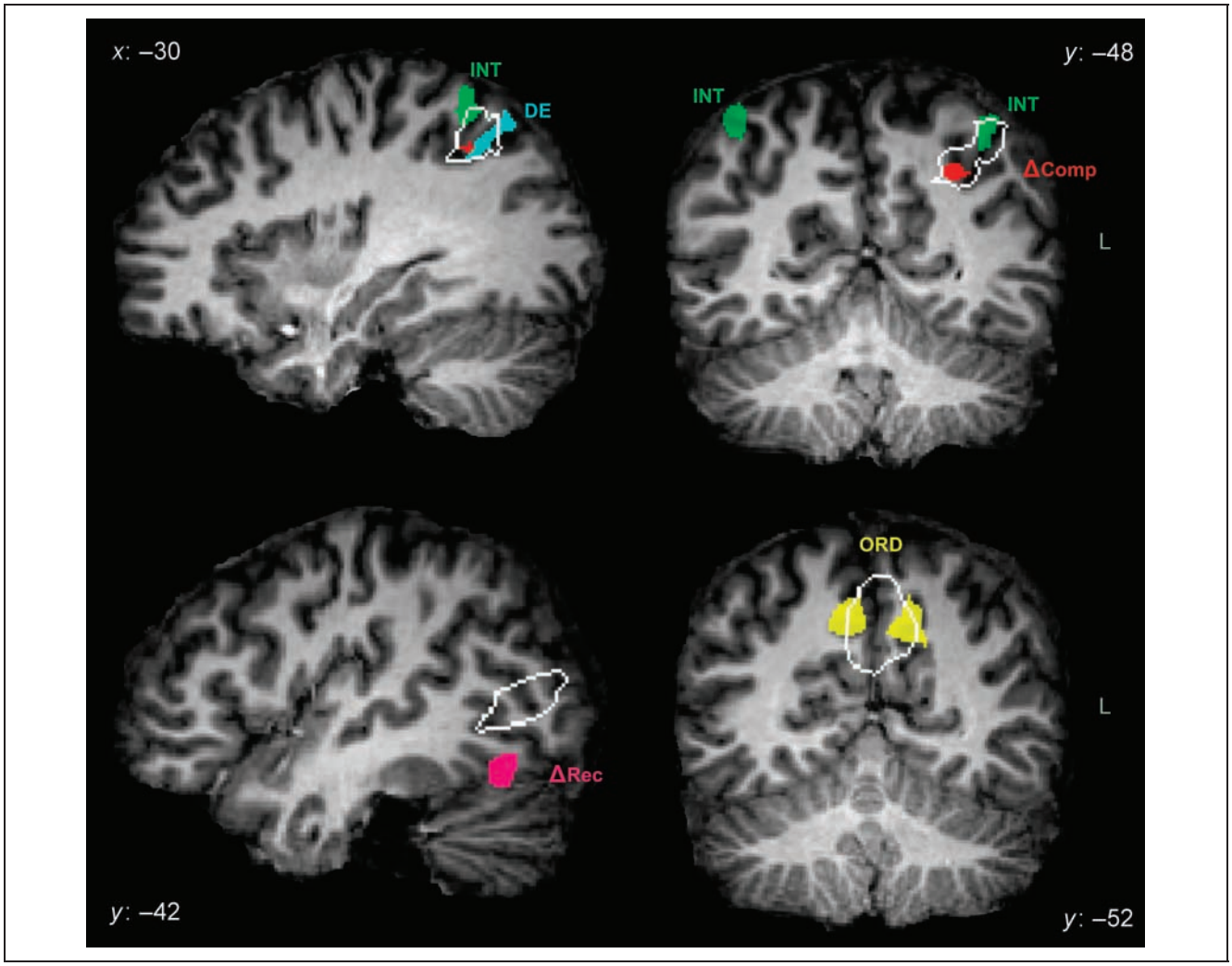

Figure 4. Regions showing a significant relation between neural activity and behavioral measures. The top two panels contain regions in the left IPS showing a relation between numerical comparison activity and numerical tasks. The left IPS region that showed overall greater activity for numerical comparison relative to recognition is outlined in white. Green regions showed a significant three-way interaction between task, stage, and scores on the postscan global-order task (labeled INT in the figure). The turquoise region showed a significant relation between subjects' distance effects on the numerical comparison task and Stage 2 comparison activity (DE). The red region showed a significant relation between changes in numerical comparison activity and changes in numerical comparison accuracy (ΔComp). The bottom left panel displays the inferior TOJ region that showed a significant relation between changes in activity and changes in accuracy for the recognition task (ΔRec). The superior region outlined in white showed greater overall activity during the recognition relative to the comparison task. These regions overlapped at the more liberal threshold of $p < .01$ ($\alpha = .01$). The bottom right panel displays regions in the precuneus (part of a post hoc analysis referred to in the Discussion). The region outlined in white showed more overall activity for the numerical comparison than the recognition task. Yellow regions showed a significant relation between Stage 2 numerical comparison activity and postscan global-order scores (ORD).

Relationship between distance effects and brain activation. The analysis of the relationship between subjects' distance effects (in terms of numerical comparison accuracy and response times) and activation during the comparison task revealed a significant positive correlation in the left IPS between Stage 2 comparison activity and Stage 2 distance effects on accuracy. Even at the reduced threshold, no other region showed a significant correlation for either measure at Stage 1 or response times at Stage 2. The IPS region found to significantly correlate with individual differences in the distance effect on accuracy is visualized in Figure 4 (shown in turquoise); region statistics are summarized in Table 4. At the ROI level, we checked whether the observed relation between distance effects and neural activity was specific to the numerical comparison task by including Stage 2 recognition task activity in the regression (i.e., Stage 2 comparison and Stage 2 recognition task activity in this region were entered as predictors of subjects' Stage 2 distance effects). When this was done, only comparison activity was found to account for a significant amount of variability in subjects' distance effects ($p < .001$). In other words, individual differences in activation of the IPS during numerical comparison, but

Table 4. A Summary of Regions Showing a Significant Relationship between Neural Activity and Behavioral Measures

	Center Gravity						
Region	*x*	*y*	*z*	*Uncorrected p Value*	*Size (mm^3)*	*Neural Measure*	*Behavioral Measure*
R. IPS	42	−49	53	.001	453	Stage-by-Task	Global Order
L. IPS	−31	−51	−50	.001	291	Stage-by-Task	Global Order
L. IPS	−26	−52	36	.005	209	Comp2 > Comp1	Δ Comp Acc.
L. Inf. TOJ	−41	−58	−10	.005	280	Rec2 > Rec1	Δ Rec Acc.
L. Caudate	−12	5	19	.005	279	Rec2 > Rec1	Δ Rec Acc.
L. IPS	−30	−59	40	.001	169	Comp2 > Base	Distance Effect

All regions were significant at the whole-brain- and cluster-level corrected at $\alpha = .01$.

not during the recognition task, accounted for a significant amount of the variability in the effect of numerical distance on accuracy.

DISCUSSION

A crucial component of mathematical competence is the ability to represent numerical quantities as abstract symbols. In the present article, we addressed the question of how numerical symbols assume their quantitative meaning through an examination of the brain regions involved in the use of recently acquired, novel numerical symbols. In particular, adult participants were trained to associate novel numerical symbols with nonsymbolic numerical quantities. By doing so, we have simulated the processes of associating abstract numerical symbols with nonsymbolic magnitudes, a process that has been proposed as underlying the development of children's understanding of the meaning of cultural symbols for the representation of numerical magnitude (Dehaene, 2008; Piazza et al., 2007; Verguts & Fias, 2004).

We identified a left-lateralized fronto-parietal network that was active when participants compared the relative numerical magnitude of the novel numerical symbols. In addition, we revealed a network engaged in processing the perceptual features of these novel numerical symbols during a perceptual recognition task. The regions identified are convergent with the predictions made by the triple-code model, which predicts separate neural pathways activate for the perceptual versus semantic processing of numerical symbols (Dehaene & Cohen, 1995). Furthermore, despite a very short training period, the regions revealed here are in keeping with those predicted by the model. To our knowledge, the present study is the first to provide evidence at the level of large-scale neural networks that corroborates these predictions for numerical symbols even at very early stages of acquisition. In addition, by investigating the relationship between individual differences in behavioral measures in symbol-learning and changes in brain activation, it was revealed that the intraparietal sulci were especially sensitive to the degree of numerical competence subjects showed in using the novel symbols.

Main Effect of Task

Comparison > Recognition Task

Regions that were more active during the numerical comparison than the perceptual recognition task comprised a left-lateralized, fronto-parietal network (Figure 3). Numerous studies involving quantity comparison of both symbolic and nonsymbolic stimuli have reported activation of the parietal lobe (Dehaene et al., 2003). In an experiment that compared several tasks thought to engage parietal cortex, the left IPS was shown to be selectively active for numerical calculation (Simon, Mangin, Cohen, Le Bihan, & Dehaene, 2002). The present data are the first to reveal that a section of the left IPS (overlapping with that identified by Simon et al.) is also engaged by the quantitative comparison of novel numerical symbols after only very brief periods of symbol training.

It should be noted that greater IPS activity for comparison relative to recognition was left-lateralized. Not until one reached the liberal threshold of $p < .05$ (uncorrected) was comparable activation seen in the right hemisphere. The specific relation between comparison accuracy and activation increases as well as that between subject distance effects and comparison activity (see below for further discussion of these correlations) were seen exclusively in the left IPS. A recent study by Piazza et al. (2007), using a neural adaptation paradigm that crossed symbolic and nonsymbolic formats, showed numerically more precise recovery for symbols in the left but not the right IPS. When dot deviants were presented among a stream of numerically repetitive Arabic numerals, neural recovery was seen for both numerically close and far deviants. In the right hemisphere, recovery was seen only for far deviants. One interpretation for this result provided by the authors is that symbols exhibited sharper numerical tuning in the left IPS. Consistent with this, Piazza, Mechelli, Price, and Butterworth (2006) showed right parietal activity for

numerical approximation and left parietal activity when subjects counted out exact numerical values (a process that depends on access to symbolic, one-to-one representations). Broadly speaking, then, our data are consistent with the notion that representation of numerical symbols depends more on the left than right parietal cortex as a function of learning.

Large activations were also seen for the comparison task in left PFC on the middle frontal gyrus (BA 6/8). Research in the domain of reading has revealed that the network of language-processing regions typically associated with reading may be augmented by direct mappings between orthography and semantic content in Chinese readers. This additional mapping process may rely on activity in the rostrolateral aspect of the activation reported here (e.g., Chen, Vaid, Bortfeld, & Boas, 2008; Siok, Niu, Jin, Perfetti, & Tan, 2008; Booth et al., 2006; Kuo et al., 2004; Siok et al., 2004). Further work connecting these literatures may provide interesting insight into symbolic representation of numerosities in that Arabic numerals, like Chinese characters, are visual representations of abstract meaning that need not carry any phonetic information. That is, both systems permit direct orthographic–semantic mappings. In addition, a large body of evidence has implicated this area in arbitrary visuomotor as well as visuovisual mappings (Chouinard & Paus, 2006; Wise & Murray, 2000; Dolan & Fletcher, 1997). As this region did not show any specific relation between individuals' activity levels and individual differences in the learning trajectory of numerical symbol learning, it is possible that the left PFC is part of a more general symbol-learning network in humans.

In this respect, recent work examining the acquisition of numerical symbols in macaque monkeys is of particular interest (Diester & Nieder, 2007). In that study, monkeys were trained to both match nonsymbolic numerosities with each other (dot–dot) and nonsymbolic numerosities with Arabic numerals (dot–symbol). The experimenters found neurons tuned to specific numerosities in both the dot–dot and the dot–symbol protocols. However, it was only in the PFC where a third population of neurons was found that responded to specific numerosities in both protocols. The presence of such ''association'' neurons in the PFC suggests that this region may play a crucial role in the mapping of numerical symbols onto nonsymbolic numerical magnitudes.

Recognition Task > Comparison

With respect to perceptual recognition of the novel symbols, a network including bilateral inferior temporal–occipital regions was shown to be more active for the perceptual recognition than the numerical comparison task. Against the background of a large body of work showing the importance of this area for complex object recognition (Grill-Spector, Kourtzi, & Kanwisher, 2001; Gauthier et al., 1999), it is plausible that the TOJ regions revealed here are involved in extracting perceptual features used to identify the previously learned symbols. This finding is also consistent with work on the word and number word form areas (McCandliss et al., 2003; Dehaene & Cohen, 1995), suggesting that perceptual recognition of novel numerical symbols, even at early stages of acquisition, may rely, in part, on these regions. Recent work suggests that recognition of written words is especially reliant on activation specifically in the left inferior temporal–occipital cortex (e.g., Vinckier et al., 2007). Intriguingly, our data showed a significant relation between accuracy increases and activation decreases across training stages in a region overlapping with that reported by Vinckier et al. (2007). This pattern of results suggests that regions known to process the visual form of words were recruited in the perceptual discrimination of these novel numerical symbols; moreover, this recruitment may have become increasingly efficient as subjects became more adept at identifying the symbols.

The Relation between Individual Differences and Brain Activation

We tested whether there were any neural regions that showed differential changes in activity between the two tasks with increased symbol training. No region showed a significant interaction. One reason for this may be that, in a given region, learning leads to activation differences in one direction for some subjects and the opposite direction in others. Thus, the mean change would appear to be at or near zero, a finding that, by itself, may mask meaningful systematic changes in neural response in that region. In light of this and due to the large behavioral differences observed in individual performance both within and between stages, we performed a series of brain–behavior analyses at the whole-brain level. The results of these analyses suggest a key role for the left and medial parietal cortices in mediating individual performance differences when acquiring novel numerical symbols.

Using postscan global-order scores as a covariate, a highly significant three-way interaction was seen in the bilateral intraparietal sulci. Analysis of the parameter estimates extracted from these parietal regions revealed that this effect was driven by a strong decrease in activity across stages for the recognition task and relatively stable activation across stages for the numerical comparison task. This resulted in a form of crossover interaction, with greater activity for recognition at Stage 1 and greater activity for comparison by Stage 2. Finally, this pattern depended on the degree to which participants accurately learned the global numerical relation between symbols, with activity in subjects showing best postscan performance most likely to exhibit this pattern of activation changes.

These results indicate that processing of numerical information in this region is at first highly dependent

on an overlap with processes important for perceptually recognizing the symbols. As this process becomes more automatic, this portion of the IPS disengages from the processes subserving the recognition and perceptual discrimination of the novel numerical symbols. An alternative explanation, however, is the observed pattern is more related to effortful processing. Those best able to eventually learn the novel symbol-quantity mappings may have first focused on recognition aspects of the task, and only after additional training did they devote greater processing resources in these regions to the symbols' numerical meaning. In other words, the first account suggests these regions increasingly become specialized in processing symbolic number, whereas the second account suggests activity in these regions is related more generally to overall processing effort.

An initial look at the behavioral data may appear to be consistent with the effortful processing interpretation. A number of subjects reached ceiling by the second stage in the recognition task, perhaps indicating a level of mastery that allowed for less effortful processing and a decrease in IPS activation. Conversely, few subjects reached ceiling in the comparison task, which may thus have required a more constant level of activation across stages. Several additional pieces of evidence, however, argue against the interaction effect being driven by a strong association between brain activation and task-related differences in performance. Behavioral performance on the recognition task did not relate to IPS neural activity during completion of this task (even at $p < .05$, uncorrected). If the decreases in recognition activity were due to some subjects reaching ceiling by the second stage, then this decrease should have been greatest for those subjects. This was not found to be the case. Indeed, the only regions showing a significant relation between recognition performance and neural activity change were the left caudate and the left TOJ.

On the other hand, behavioral measures from the numerical comparison task did bear a strong positive relation to activity levels in several subregions of the left IPS. Here, individuals who showed the greatest performance improvements were also those who showed the greatest activation increase in the left IPS. These data suggest that it is performance improvement on the comparison task, rather than improvement on the recognition task, that is associated with relative levels of activation in the left IPS. Taken together, these factors support the view that the interaction observed in the present study between postscan performance and differential change in activation levels for the two tasks is most likely explained by increasing specialization of this left parietal region for the representation and processing of the numerical magnitudes associated with the novel symbols. Importantly, this specialization varies substantially between individuals and was found to be greatest in those individuals who had the highest scores on the postscan ordering task (which required them to correctly order all six symbols in ascending numerical order).

Further support for the notion that individual differences in semantic association between novel numerical symbols and their nonsymbolic referents are strongly related to activity in the left IPS comes from the finding that a subregion of the left IPS showed a strong positive correlation with the degree of performance *improvement* exhibited by individual subjects (Figure 4, shown in red). In other words, those individuals who showed relatively large performance increases were also those who showed the greatest levels of activation increase in the left IPS. This relationship was seen only for the numerical comparison and not the recognition task (even at $p < .05$, uncorrected). As participants significantly improved in accuracy performance across stages in both tasks, the fact that the relation between neural and behavioral change in this region was specific to the symbol-comparison task suggests our observation of this region was not due to general learning-related effects that might be shared between the recognition and comparison tasks.

Why should increased learning of numerical symbols be associated with greater engagement of the parietal cortex? A recent review of the literature on the cognitive neuroscience of learning (Kelly & Garavan, 2005) suggests that both increases and decreases in activation can be found as a consequence of learning and that the specific direction depends on the particular domain that is being practiced. With respect to numerical learning in the IPS in particular, this region has been implicated in the representation and processing of numerical magnitude across a large body of studies. It is therefore reasonable to suggest that this region comes to represent symbolic numerical magnitude as a function of experience and learning. Indeed, recent developmental neuroimaging studies have revealed age-related increases in the recruitment of the parietal cortex during symbolic and nonsymbolic magnitude processing as well as during calculation (Ansari & Dhital, 2006; Ansari et al., 2005; Rivera et al., 2005). Furthermore, recent evidence (Grabner et al., 2007) has revealed that individuals with relatively higher mathematical competence recruit parietal regions to a greater extent than their less able peers. Against this background, it is plausible that increased experience, learning, and practice, as well as levels of competence, are positively rather than negatively associated with increasing activation of the parietal cortex.

An adjacent region of the left IPS showed a strong positive relationship between symbol-comparison activity levels and the behavioral distance effects on accuracy observed across participants. This finding is consistent with previous neuroimaging studies that have found an effect of numerical distance in similar lateral parietal areas (Pinel et al., 2001) and further supports the interpretation that greater activation in this region for numerical comparison relative to recognition of newly acquired

numerical symbols reflects the acquisition of numerically meaningful content.

It is important to point out in this context that the existing literature has looked at the relation between numerical distance and neural activity using symbols that have already acquired their numerical meaning (Piazza et al., 2007; Ansari, Dhital, & Siong, 2006; Liu, Wang, Corbly, Zhang, & Joseph, 2006; Kaufmann et al., 2005; Szucs & Csepe, 2005; Pinel et al., 2001), whereas here we are looking at the effect of distance during the comparison of symbols that are in the process of being mapped onto their semantic referents (numerical magnitudes). This important difference might explain why in studies using Arabic numerals a negative correlation between numerical distance and fMRI signal was obtained, whereas here we report a positive correlation between IPS activation and individual differences in the distance effect. In the current study, accuracy performance as a whole improved with training, and the distance effect showed an increasing trend as well. Thus, the distance effect emerged as a function of training. In particular, when entered together as predictors of overall changes in numerical comparison accuracy, IPS activation increases in LD accuracy remained a significant predictor [$t(19) = 3.55$, $p = .002$], whereas SD accuracy did not [$t(19) = 0.98$, $p = .341$]. Therefore, at such an early stage of acquisition, LD comparisons are the better predictor of numerical symbol-learning, and thus would appear to be the better indicator of the extent to which subjects access representations of numerical quantity associated with newly acquired numerical symbols in the IPS.

It is also important to note that the observed neurobehavioral correlations were between measures of accuracy and fMRI beta values; a similar relationship between response times and neural activity was not observed. This result is perhaps not surprising in that the training regime employed here was not of sufficient duration for performance using the symbols to have become uniformly automated across participants. This was intended to be the case so that meaningful individual differences could be captured. In view of this, accuracy change in the present context may represent a better index of individual performance differences than response-time changes.

The symbol-comparison task also activated an extensive area within the precuneus. A recent systematic review of neuroimaging papers reporting activation of the precuneus indicates that the more anterior aspect of the precuneus is often involved in tasks requiring mental imagery, especially for the mental manipulation of spatial relations (Cavanna & Trimble, 2006). It has long been argued that numerical representations are highly spatial in nature (for recent reviews, see Hubbard, Piazza, Pinel, & Dehaene, 2005; Walsh, 2003). It is plausible then that relations between the symbols (i.e., their relative order) may have been mapped using some form of spatial imagery, a process possibly driven, to some extent, by activity in the precuneus. Consistent with this view, Stage 2 comparison activity in the precuneus was strongly related to accuracy on the postscan global-ordering task [right: Tal(10,−52,37), $r(19) = .737$, $p < .001$; left: Tal(−10,−52,36), $r(19) = .750$, $p < .001$; both regions whole-brain cluster-level corrected at $\alpha = .01$; shown in yellow in Figure 4].

The present study is not the first to show the precuneus to be active in numerical tasks (e.g., Ansari et al., 2006; Pinel et al., 2001). In addition, Van Opstal et al. (2008) recently used fMRI to examine the neural correlates of learning to acquire ordering relations between novel shapes. In that study, participants underwent several training stages wherein they made binary comparisons, deciding which of two novel shapes preceded the other in terms of relative order. As feedback was provided after each trial, participants were eventually able to correctly identify pairwise relative order in this way. When the authors compared activity during the last relative to the third-to-last round of comparisons, greater activity for the lattermost round was seen in several parietal regions, key among which were the precuneus and the left angular gyrus. The present data are therefore consistent with an important role for the precuneus in the processing of ordinal relationships.

It should be noted that although Van Opstal et al. (2008) and indeed many other researchers (for a review, see Suzuki, 2008) have observed associative learning-related changes in the medial-temporal lobes (MTLs), this was not the case in the present study. We can only speculate as to why no such changes were observed here. It is possible that the relatively short training in the present study did not lead to significant changes related to consolidation of associations in MTL structures. In other words, it is possible that MTL regions were active at both stages of learning. Future studies should investigate whether the type of training used here leads to significant changes in the MTL after longer periods of training.

Conclusions

The present findings reveal a segregation of the neural networks involved in processing semantic meaning and perceptual features of novel numerical symbols after only a short training period. Specifically, a left-lateralized network of fronto-parietal regions was found to be activated during comparison of the novel symbols in terms of their numerical magnitude. In contrast, right frontal and bilateral temporal–occipital junction regions were significantly more engaged during recognition of the novel symbols in terms of their perceptual features. An analysis of individual differences revealed a relationship in the bilateral intraparietal sulci between increasing segregation of neural activity during numerical and perceptual processing, and individual differences in learning the novel symbols' global numerical order. Specifically, increasing segregation was seen in activation of the left IPS

between numerical comparison and perceptual recognition of the novel symbols as a function of increased training. The degree of increasing segregation was positively related to performance on a postscan measure of participants' ability to correctly place the novel symbols in their overall numerical order. Moreover, left hemisphere activity in the IPS showed a further significant relationship between changes in numerical comparison (but not recognition) performance and neural activity. Finally, left IPS activity was also significantly related to subjects' numerical distance effects when comparing novel symbols. Taken together, these findings provide converging evidence that the left parietal cortex plays an important role in the degree to which individuals learn to associate novel symbols with their numerical referents. Furthermore, the present data suggest an important role of the precuneus in learning the relative order of novel numerical symbols. Against the background of these findings, future studies should investigate the extent to which the learning-related changes observed here converge with those underlying the acquisition of symbolic numerical meaning over developmental time.

Reprint requests should be sent to Daniel Ansari, Department of Psychology, University of Western Ontario, Westminster College, 361 Winderemere Road, London, Ontario, Canada N6G 2K3, or via e-mail: daniel.ansari@uwo.ca.

REFERENCES

Ansari, D. (2008). Effects of development and enculturation on number representation in the brain. *Nature Reviews Neuroscience, 9,* 278–291.

Ansari, D., & Dhital, B. (2006). Age-related changes in the activation of the intraparietal sulcus during nonsymbolic magnitude processing: An event-related functional magnetic resonance imaging study. *Journal of Cognitive Neuroscience, 18,* 1820–1828.

Ansari, D., Dhital, B., & Siong, S. C. (2006). Parametric effects of numerical distance on the intraparietal sulcus during passive viewing of rapid numerosity changes. *Brain Research, 1067,* 181–188.

Ansari, D., Garcia, N., Lucas, E., Hamon, K., & Dhital, B. (2005). Neural correlates of symbolic number processing in children and adults. *NeuroReport, 16,* 1769–1773.

Bitan, T., Booth, J. R., Choy, J., Burman, D. D., Gitelman, D. R., & Mesulam, M. M. (2005). Shifts of effective connectivity within a language network during rhyming and spelling. *Journal of Neuroscience, 25,* 5397–5403.

Bitan, T., Manor, D., Morocz, I. A., & Karni, A. (2005). Effects of alphabeticality, practice and type of instruction on reading an artificial script: An fMRI study. *Brain Research, Cognitive Brain Research, 25,* 90–106.

Booth, J. R., Lu, D., Burman, D. D., Chou, T. L., Jin, Z., Peng, D. L., et al. (2006). Specialization of phonological and semantic processing in Chinese word reading. *Brain Research, 1071,* 197–207.

Callan, A. M., Callan, D. E., & Masaki, S. (2005). When meaningless symbols become letters: Neural activity change in learning new phonograms. *Neuroimage, 28,* 553–562.

Cavanna, A. E., & Trimble, M. R. (2006). The precuneus: A review of its functional anatomy and behavioural correlates. *Brain, 129,* 564–583.

Chen, H. C., Vaid, J., Bortfeld, H., & Boas, D. A. (2008). Optical imaging of phonological processing in two distinct orthographies. *Experimental Brain Research, 184,* 427–433.

Chouinard, P. A., & Paus, T. (2006). The primary motor and premotor areas of the human cerebral cortex. *Neuroscientist, 12,* 143–152.

Dehaene, S. (1997). *The number sense: How the mind creates Mathematics*. New York: Oxford University Press.

Dehaene, S. (2008). Symbols and quantities in parietal cortex: Elements of a mathematical theory of number representation and manipulation. In P. Haggard, Y. Rossetti, & M. Kawato (Eds.), *Sensorimotor foundations of higher cognition (attention and performance)* (pp. 527–574). New York: Oxford University Press.

Dehaene, S., & Changeaux, J. P. (1993). Development of elementary numerical abilities—A neuronal model. *Journal of Cognitive Neuroscience, 5,* 390–407.

Dehaene, S., & Cohen, L. (1995). Towards an anatomical and functional model of number processing. *Mathematical Cognition, 1,* 83–120.

Dehaene, S., Piazza, M., Pinel, P., & Cohen, L. (2003). Three parietal circuits for number processing. *Cognitive Neuropsychology, 20,* 487–506.

Diester, I., & Nieder, A. (2007). Semantic associations between signs and numerical categories in the prefrontal cortex. *PLoS Biology, 5,* e294.

Dolan, R. J., & Fletcher, P. C. (1997). Dissociating prefrontal and hippocampal function in episodic memory encoding. *Nature, 388,* 582–585.

Forkstam, C., & Petersson, K. M. (2005). Towards an explicit account of implicit learning. *Current Opinion in Neurology, 18,* 435–441.

Forman, S. D., Cohen, J. D., Fitzgerald, M., Eddy, W. F., Mintun, M. A., & Noll, D. C. (1995). Improved assessment of significant activation in functional magnetic resonance imaging (fMRI): Use of a cluster-size threshold. *Magnetic Resonance in Medicine, 33,* 636–647.

Friston, K. J., Fletcher, P., Josephs, O., Holmes, A., Rugg, M. D., & Turner, R. (1998). Event-related fMRI: Characterizing differential responses. *Neuroimage, 7,* 30–40.

Friston, K. J., Holmes, A. P., Worsley, K. J., Poline, J. P., Frith, C. D., & Frackowiak, R. S. J. (1995). Statistical parametric maps in functional imaging: A general linear approach. *Human Brain Mapping, 2,* 189–210.

Gauthier, I., Tarr, M. J., Anderson, A. W., Skudlarski, P., & Gore, J. C. (1999). Activation of the middle fusiform ''face area'' increases with expertise in recognizing novel objects. *Nature Neuroscience, 2,* 568–573.

Gauthier, I., Williams, P., Tarr, M. J., & Tanaka, J. (1998). Training ''greeble'' experts: A framework for studying expert object recognition processes. *Vision Research, 38,* 2401–2428.

Goebel, R., Esposito, F., & Formisano, E. (2006). Analysis of functional image analysis contest (FIAC) data with brainvoyager QX: From single-subject to cortically aligned group general linear model analysis and self-organizing group independent component analysis. *Human Brain Mapping, 27,* 392–401.

Grabner, R. H., Ansari, D., Reishofer, G., Stern, E., Ebner, F., & Neuper, C. (2007). Individual differences in mathematical competence predict parietal brain activation during mental calculation. *Neuroimage, 38,* 346–356.

Grill-Spector, K., Kourtzi, Z., & Kanwisher, N. (2001). The lateral occipital complex and its role in object recognition. *Vision Research, 41,* 1409–1422.

Hubbard, E. M., Piazza, M., Pinel, P., & Dehaene, S. (2005). Interactions between number and space in parietal cortex. *Nature Reviews Neuroscience, 6,* 435–448.

Kaufmann, L., Koppelstaetter, F., Delazer, M., Siedentopf, C., Rhomberg, P., Golaszewski, S., et al. (2005). Neural correlates of distance and congruity effects in a numerical Stroop task: An event-related fMRI study. *Neuroimage, 25,* 888–898.

Kelly, A. M., & Garavan, H. (2005). Human functional neuroimaging of brain changes associated with practice. *Cerebral Cortex, 15,* 1089–1102.

Kuo, W. J., Yeh, T. C., Lee, J. R., Chen, L. F., Lee, P. L., Chen, S. S., et al. (2004). Orthographic and phonological processing of Chinese characters: An fMRI study. *Neuroimage, 21,* 1721–1731.

Liu, X., Wang, H., Corbly, C. R., Zhang, J., & Joseph, J. E. (2006). The involvement of the inferior parietal cortex in the numerical Stroop effect and the distance effect in a two-digit number comparison task. *Journal of Cognitive Neuroscience, 18,* 1518–1530.

McCandliss, B. D., Cohen, L., & Dehaene, S. (2003). The visual word form area: Expertise for reading in the fusiform gyrus. *Trends in Cognitive Sciences, 7,* 293–299.

Moyer, R. S., & Landauer, T. K. (1967). Time required for judgements of numerical inequality. *Nature, 215,* 1519–1520.

Piazza, M., Mechelli, A., Price, C. J., & Butterworth, B. (2006). Exact and approximate judgements of visual and auditory numerosity: An fMRI study. *Brain Research, 1106,* 177–188.

Piazza, M., Pinel, P., Le Bihan, D., & Dehaene, S. (2007). A magnitude code common to numerosities and number symbols in human intraparietal cortex. *Neuron, 53,* 293–305.

Picard, N., & Strick, P. L. (2001). Imaging the premotor areas. *Current Opinion in Neurobiology, 11,* 663–672.

Pinel, P., Dehaene, S., Riviere, D., & LeBihan, D. (2001). Modulation of parietal activation by semantic distance in a number comparison task. *Neuroimage, 14,* 1013–1026.

Price, C. J., & Mechelli, A. (2005). Reading and reading disturbance. *Current Opinion in Neurobiology, 15,* 231–238.

Rivera, S. M., Reiss, A. L., Eckert, M. A., & Menon, V. (2005). Developmental changes in mental arithmetic: Evidence for increased functional specialization in the left inferior parietal cortex. *Cerebral Cortex, 15,* 1779–1790.

Simon, O., Mangin, J. F., Cohen, L., Le Bihan, D., & Dehaene, S. (2002). Topographical layout of hand, eye, calculation, and language-related areas in the human parietal lobe. *Neuron, 33,* 475–487.

Siok, W. T., Niu, Z., Jin, Z., Perfetti, C. A., & Tan, L. H. (2008). A structural–functional basis for dyslexia in the cortex of Chinese readers. *Proceedings of the National Academy of Sciences, U.S.A., 105,* 5561–5566.

Siok, W. T., Perfetti, C. A., Jin, Z., & Tan, L. H. (2004). Biological abnormality of impaired reading is constrained by culture. *Nature, 431,* 71–76.

Suzuki, W. A. (2008). Associative learning signals in the brain. *Progress in Brain Research, 169,* 305–320.

Szucs, D., & Csepe, V. (2005). The effect of numerical distance and stimulus probability on ERP components elicited by numerical incongruencies in mental addition. *Brain Research, Cognitive Brain Research, 22,* 289–300.

Talairach, J., & Tournoux, P. (1988). *Co-planar stereotaxic atlas of the human brain: 3-Dimensional proportional system: An approach to cerebral imaging*. New York: Thieme Medical Publishers.

Van Opstal, F., Verguts, T., Orban, G. A., & Fias, W. (2008). A hippocampal–parietal network for learning an ordered sequence. *Neuroimage, 40,* 333–341.

Verguts, T., & Fias, W. (2004). Representation of number in animals and humans: A neural model. *Journal of Cognitive Neuroscience, 16,* 1493–1504.

Vinckier, F., Dehaene, S., Jobert, A., Dubus, J. P., Sigman, M., & Cohen, L. (2007). Hierarchical coding of letter strings in the ventral stream: Dissecting the inner organization of the visual word-form system. *Neuron, 55,* 143–156.

Walsh, V. (2003). A theory of magnitude: Common cortical metrics of time, space and quantity. *Trends in Cognitive Sciences, 7,* 483–488.

Wise, S. P., & Murray, E. A. (2000). Arbitrary associations between antecedents and actions. *Trends in Neurosciences, 23,* 271–276.

Xue, G., Chen, C., Jin, Z., & Dong, Q. (2006). Language experience shapes fusiform activation when processing a logographic artificial language: An fMRI training study. *Neuroimage, 31,* 1315–1326.